

## Study on Cloud Classifications by using AVHRR, GMS-5 and Terra/MODIS satellite data\*

SHI Chunxiang (师春香) ZHANG Wenjian (张文建)

GUO Wei (郭伟) ZHANG Liyang (张里阳)

(National Satellite Meteorological Center, China meteorological Administration, Beijing, 100081, PRC [shicx@nsmc.cma.gov.cn](mailto:shicx@nsmc.cma.gov.cn))

### ABSTRACT

This paper presents the automated pixel-scale neural network classification methods being developed at National Satellite Meteorological Center (NSMC) of China to classify clouds by using NOAA/AVHRR and GMS-5 satellite imageries. By using Terra satellite MODIS imageries, a automated pixel-scale threshold techniques has been developed to detect and classify clouds. The study focuses on applications of these cloud classification techniques to the HUIHE and the Yangtze River drainage basin. The different types of clouds show more clearly on this cloud classification image than single band image. The results of the cloud classifications are the basis of studying cloud amount, cloud top height and cloud top pressure. Cloud mask methods are widely used in SST, LST, and TPW retrieval schemes. Some case studies about cloud mask and cloud classification in satellite imageries, which relate with the study of Global Energy and Water Cycle Experiment (GEWEX) in the HUIHE and the Yangtze River drainage basin are illustrated.

**Key words:** cloud mask and classification, neural network, satellite imagery, MODIS data.

### 1. INTRODUCTION

Cloud mask algorithms are based on the fact that the spectral behavior of clouds and earth surfaces are different in window channels. Higher reflectance and lower temperature than the underlying earth surface generally characterize clouds. The main difficulties of cloud detecting are that the earth surface characteristics (which varies with the surface type, the atmospheric conditions, the sun and satellite respective positions) is very complex so that the contrast between the cloud and earth surface characteristics may be very low under certain circumstances. In addition, some cloud types such as thin cirrus, low stratus at night, and small cumulus are difficult to detect because of insufficient contrast with the surface radiance. Cloud edges cause further difficulty since the instrument field of view will not always be completely cloudy or clear.

Three techniques may be applied to cloud detection. Clustering techniques, which are scene dependent methods, mainly use pixel values of the entire scene through histogram analysis or other calculations to segment the image according to pre-defined rules; Artificial neural networks, the advanced multidimensional regression techniques, are capable of treating predictions and predictors in a very flexible way (allowing nonlinear relations). Multi-spectral threshold techniques are based on pixel-by-pixel analysis of radiance where cloud-free and cloudy pixels are identified if pixel radiance pass a sequence of threshold tests. The chosen method should be

---

\* This Work is Supported by the National Science Foundation of China(49794030)

efficient in term of computing time, make the maximum use of channels, be easily adapted (e.g., if one channel is missing), and be mature. Moreover, it should be possible to easily tune the algorithm. The clustering techniques have been considered to be too scene-dependant. Artificial neural network techniques are promising methods, but it is sensitive to the learning data set<sup>[1][2][3]</sup>. One of the main advantage of the multi-spectral threshold technique is that it is relatively easy to adapt thresholds to varying meteorological conditions, earth surface types, viewing geometry using external data, for example, Numerical Weather Prediction (NWP) model forecasting, Radiation Transfer Model (RTM) calculations, climatological atlas<sup>[4][5][6]</sup>. This physical approach will also allow an easy tuning of the cloud mask prototypes to other spectral characteristics. One of the main disadvantages is that the thresholds need to be tuned frequently.

This paper first presents the automated pixel-scale neural network methods being developed in NSMC to do cloud detection and cloud classification. The data set used in this study are mainly from Advanced Very High Resolution Radiometer (AVHRR), the Geostationary Meteorological Satellite (GMS) imageries. Then the automated pixel-scale threshold cloud detection and classification technique is presented by using Earth Observation Satellite (EOS) Moderate Resolution Imaging Spectrometer (MODIS) imageries.

## 2. NOAA/AVHRR NEURAL NETWORK CLOUD CLASSIFICATION TECHNIQUES

The field of neural networks can be thought of as being related to artificial intelligence, machine learning, parallel processing, statistics, and other fields. The attraction of neural networks is that they are best suited to solving the problems that are the most difficult to solve by traditional computational methods. We use the Back-Propagation (BP) neural network in this cloud classification study, which is used widely in many fields.

The BP learning process works in small iterative steps: one of the example cases is applied to the network, and the network produces some output based on the current state of it's synaptic weights (initially, the output will be random). This output is compared to the known-good output, and a mean-squared error signal is calculated. The error value is then propagated backwards through the network, and small changes are made to the weights in each layer. The weight changes are calculated to reduce the error signal for the case in question. The whole process is repeated for each of the example cases, then back to the first case again, and so on. The cycle is repeated until the overall error value drops below some pre-determined thresholds. At this point we say that the network has learned the problem "well enough" - the network will never exactly learn the ideal function, but rather it will asymptotically approach the ideal function.

AVHRR has five channels of visible, near-infrared, and thermal infrared spectrum. The channels spectrum characteristics are: channel 1, 0.58-0.68  $\mu$  m, channel 2, 0.725-1.10  $\mu$  m, channel 3, 3.55-3.93  $\mu$  m, channel 4, 10.3-11.3  $\mu$  m and channel 5, 11.5-12.5  $\mu$  m, respectively. The AVHRR Global Area Coverage (GAC) data provides collection of data from all spectral channels for global, and world wide users can receive HRPT direct broadcasting data stream locally. Each pass of the satellite provides a 2399 km (1491m) wide swath. The satellite orbits the earth and measures the temperature of clouds and the sea surface. The AVHRR applications have extended far beyond these original objectives, however, simple mapping of cloud patterns is still an important application, especially at high latitudes where data from geostationary satellites are

severely distorted (due to earth curvature).

In this study, the sample database of clouds, land and water is built based on AVHRR 5 channels data which includes more than thirty thousands 8\*8 pixels samples and more than twenty thousands one pixel samples. Theory analysis and experiment show that not only 5 channel data can be used to distinguish clouds and land and water but also the band combination with each other can do so. For example, the differences of AVHRR channel 4 and 5 can be used to distinguish water particle cloud and ice particle cloud because the biggest absorption difference between water particles and ice particles is near 12 μ m. Based on theory analyses and experiments, 80 features are extracted from 5 channels AVHRR data for 8\*8 pixels samples, which involve spectrum features, gray features, channel difference features and the gray scale statistical features. 20 features are selected using step-by-step distinguish analysis method, which includes spectrum features, gray features. 20 features are extracted from 5 channel AVHRR data for single pixel samples.

The inputs of our AVHRR automatic cloud classification system are 5 AVHRR channels data and outputs are classified gray image. Cloud classified image involves cumulonimbus, cumulus congestus, cumulus, cirrus, middle cloud, low cloud and land, water and unknown pixel.

Cloud classification experiment of sample database is done using neural network method. This neural network model has 20 input nodes, 2 hidden layers and 4 output nodes (20-40-15-4). More than three thousands samples selected randomly are used to train the neural network model. The other independent samples are used for testing. Testing result shows classification accuracy is about 78% for single pixel sample database and 79% for 8\*8 pixels samples database. Table 1 shows classification experiment results. Although classification accuracy of 8\*8 pixels samples is a little better than single pixel sample, but when neural network model is used in the practical application to one satellite image single pixel cloud classification neural network model is better.

**Table 1.** Single pixel cloud classification experiment results

Calculation Fact	1	2	3	4	5	6	7	8	9	Right sample numbers	Total numbers of each types	Accurate ratio %
1	2207	157	25	335	21	0	0	0	45	2207	2835	77.0
2	158	1119	41	457	0	0	0	0	158	1119	2091	53.0
3	29	3	684	76	133	223	121	0	0	684	1269	53.0
4	145	214	3	7186	435	0	3	0	194	7186	8374	85.0
5	38	6	10	450	1822	1	47	0	13	1822	2400	75.0
6	8	0	554	107	126	1648	413	0	0	1648	2856	57.0
7	1	0	5	0	2	0	1935	33	6	1935	1982	97.0
8	0	1	2	0	1	1	28	330	13	330	376	87.0
Total Accurate ratio of cloud classification						77.8%						

Figure 1 is a clouds classification case study using trained neural network model, figure 1(a) is classified color image of NOAA-11 at 5:00 on July 20 in 1992 (UTC), the region is 30° ~35° N, 140° ~145° E, it located the north-east region of HUBEX experiment area. figure 1(b) is channel 4 cloud image at the same time. In this case, cumulonimbus (red), cumulus congestus (purple), cumulus humilis (light purple), cirrus (cyan), middle cloud (yellow), low cloud (pink), land (green), water (blue), and unknown (black) is marked. But some of multiple level clouds and boundary pixels are not recognized because of having no such samples in learning sample set.

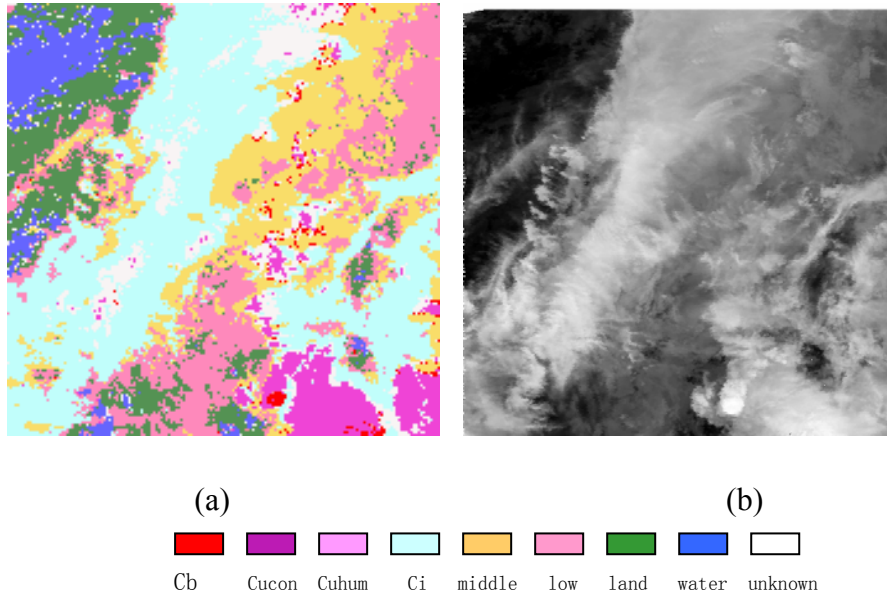


Figure 1. Cloud and surface classification case study.

Figure 1(a) is NOAA-11 at 5 on July 20 in 1992 (UTC), the region is 30' ~35' N, 140' ~145' E classified color image, figure 1(b) is channel 4 cloud image at the same time.

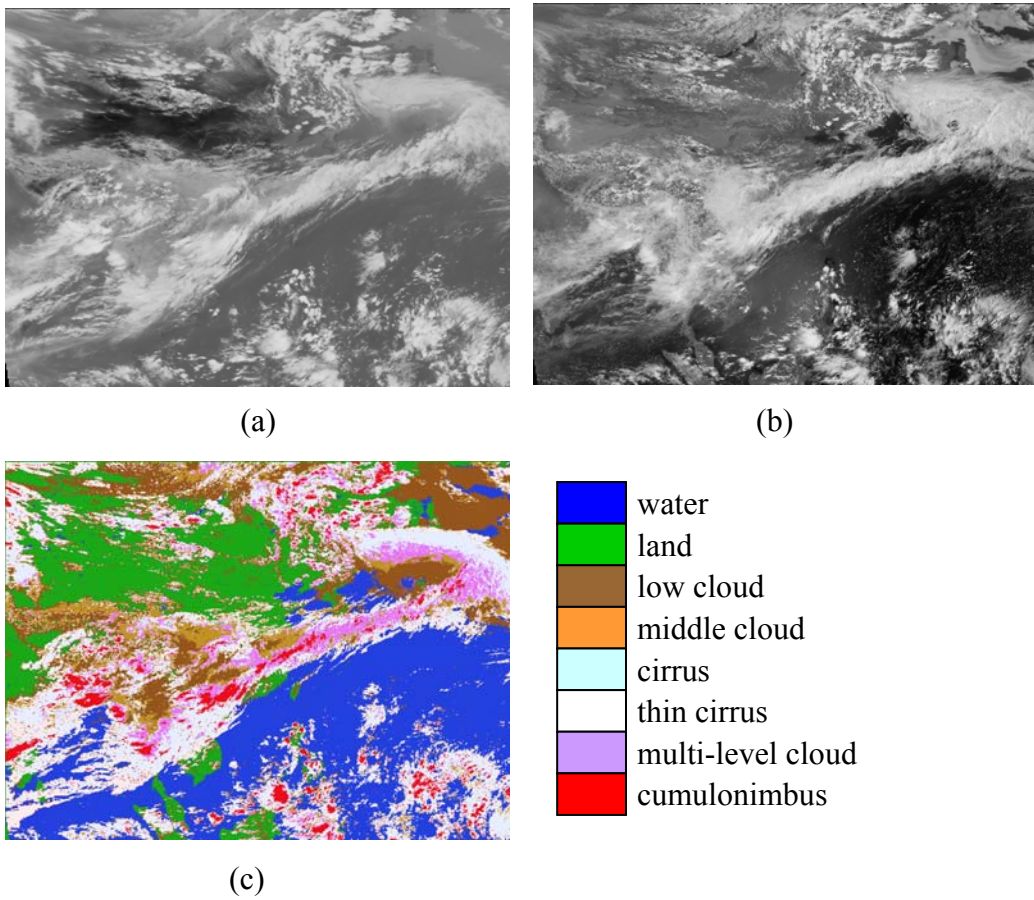


Figure 2. 1999062406 GMS-5 IR1(a), VIS(b) and classified color image(c)

### 3. GMS-5 NEURAL NETWORK CLOUD CLASSIFICATION TECHNIQUES

The GMS series are satellites in geostationary orbit at 140° east longitude. Monitoring weather conditions, they are one link in World Weather Watch sponsored by the World Meteorological Organization. Observation data consisting of cloud distribution pictures sent from these satellites is used in many fields including TV and newspaper weather forecasts. GMS-5 has four channels of visible and thermal infrared spectrum. The channels spectrum characteristics are: channel 1, 0.55-0.90  $\mu$  m, channel 2, 6.5-7.0  $\mu$  m, channel 3, 10.5-11.5  $\mu$  m, channel 4, 11.5-12.5  $\mu$  m.

Sample database of clouds, land and water is built based on GMS-5 four channels data which includes several thousands of one pixel samples. Sample database is also collected from the GMS-5 satellite imagery from June to August in 1998. GMS-5 has two window channels with little atmospheric absorption. They can show thermal characters of surface well. The water vapor channel detects middle-high level water vapor in the atmosphere. Additionally there is a visible band. Theory analysis and experiment show that not only four channels data can be used to distinguish clouds and lands and water but also the difference between channels can do so. For example, the brightness temperature difference between channel 3 and channel 4 can be used to distinguish thin cirrus. On the basis of theory analyses and experiment, 20 features are selected as the input of the cloud classification neural network model.

Figure 2 is a clouds classification case study using trained neural network model, Figure 2(a) is infrared (channel 3) satellite imagery of GMS-5 at 6:00 on June 24 in 1999 (UTC), the region is 0° ~60° N, 70° ~150° E. Figure 2(b) is the visible (channel 1) satellite imagery at the same time. Figure 2(c) is GMS-5 cloud classified color image at the same time. In this case, water, land, low-level cloud, middle-level cloud, multi-level cloud, cirrus and cumulonimbus are showed with different color. The low-level cloud in the up-right of the imagery is clearly shown in the classification image but it is hard to be distinguished in the infrared imagery. Over the HUIHE and the Yangtze Rive drainage basin there are a MEIYU front cloud system lasted from June 22 to July 3.

### 4. MODIS CLOUD MASK AND CLOUD CLASSIFICATION USING MULTI-SPECTRAL THRESHOLDING TECHNIQUE

#### 4.1 MODIS DATA

The 36 channel MODIS data offers the opportunity for multi-spectral approaches to cloud mask and cloud classification more accurately. The spectrum characteristics of the 36 channels are shown in table 2. MODIS cloud mask and classification algorithm is very complex.

#### 4.2 CLOUD MASK AND CLASSIFICATION METHODS FOR MODIS

The multi-spectrum threshold algorithm is applied to MODIS imagery for cloud mask and classification. For nomenclature, we shall denote the satellite measured solar reflectance as  $R$ , and refer to the infrared radiance as brightness temperature (equivalent blackbody temperature determined using the Planck function) denoted as  $BT$ . Subscripts refer to the wavelength at which the measurement is made. The multiple thresholds cloud mask and cloud classification algorithm

is to start with single pixel (1000m field of view) tests. Thresholds are changed with space and time.

#### 4.2.1 CHARACTERISTIC ANALYSIS ABOUT SOME OF THE MODIS BANDS

MODIS has a unique capability since it has measurements at three wavelengths in the window, 8.6, 11, and 12  $\mu$  m. Three spectral regions mentioned are very useful in determination of

**Table 2.** MODIS bands used in the MODIS cloud mask algorithm.

Band	Wavelength(mm)	Used in Cloud Mask	
1 (250 m)	0.659	Y	(250 m and 1 km) clouds, shadow
2 (250 m)	0.865	Y	(250 m and 1 km) low clouds
3 (500 m)	0.470	N	
4 (500 m)	0.555	Y	snow
5 (500 m)	1.240	Y	shadow
6 (500 m)	1.640	Y	snow
7 (500 m)	2.130	Y	aerosol
8	0.415	N	
9	0.443	N	
10	0.490	N	
11	0.531	N	
12	0.565	N	
13	0.653	N	
14	0.681	N	
15	0.750	N	
16	0.865	N	
17	0.905	N	
18	0.936	Y	low cloud
19	0.940	Y	shadow
20	3.750	Y	cloud
21/22	3.959	N(21)/Y(22)	window, shadow
23	4.050	Y	shadow
24	4.465	N	
25	4.515	N	
26	1.375	Y	thin cirrus
27	6.715	Y	high cloud
28	7.325	N	
29	8.550	Y	cloud
30	9.730	N	
31	11.030	Y	cloud
32	12.020	Y	cloud
33	13.335	N	
34	13.635	N	
35	13.935	Y	high cloud
36	14.235	N	

cloud free atmospheres. Because the index of refraction varies quite markedly over this spectral region for water, ice, and minerals common to many naturally occurring aerosols, the effect on the brightness temperature of each of the spectral regions is different, depending on the absorbing constituent.

As a result of the relative spectral uniformity of surface emittance in the IR, spectral tests within various atmospheric windows (such as bands 29, 31, 32 at 8.6, 11, and 12  $\mu$  m, respectively) can be used to detect the presence of cloud. Differences between *BT11* and *BT12* are widely used for cloud screening with AVHRR measurements, and this technique is often referred to as the split window technique. Saunders and Kriebel(1988)<sup>[7]</sup> used *BT11* - *BT12* differences to detect cirrus clouds----brightness temperature differences are greater over thin clouds than over clear or overcast conditions. Cloud thresholds are set as a function of satellite zenith angle and the *BT11*

brightness temperature. <sup>[8][9]</sup>

In difference techniques, the measured radiance at two wavelengths are converted to brightness temperatures and subtracted. Because of the wavelength dependence of optical thickness and the non-linear nature of the Planck function ( $BT$ ), the two brightness temperatures are often different. The basis of the split window and tri-spectral technique for cloud mask lies in the differential water vapor absorption that exists between different window channel (8.6 and 11  $\mu$  m and 11 and 12  $\mu$  m) bands. These spectral regions are considered to be part of the atmospheric window, where absorption is relatively weak. Most of the absorption lines are a result of water vapor molecules, with a minimum occurring around 11  $\mu$  m. Since the absorption is weak,  $BT_{11}$  can be corrected for moisture absorption by adding the scaled brightness temperature difference of two spectrally close channels with different water vapor absorption coefficients; the scaling coefficient is a function of the differential water vapor absorption between the two channels. This is the basis for sea surface temperature (SST) retrieval.

A tri-spectral combination of observations at 8.6, 11 and 12  $\mu$  m is suggested for detecting cloud properties by Ackerman *et al.* (1990) <sup>[10]</sup>. Strabala *et al.* (1994) <sup>[11]</sup> further explored this technique by utilizing very high spatial-resolution data from MAS (MODIS Airborne Simulator). The physical premise of the technique is that ice and water vapor absorption peak in opposite halves of the window region; so that positive 8.6 minus 11  $\mu$  m brightness temperature differences indicate cloud while negative differences, over oceans, indicate clear regions. The relationship between the two brightness temperature differences and clear-sky have also been examined using collocated HIRS (High Resolution Infrared Radiation Sounder) and AVHRR GAC global ocean data sets. As the atmospheric moisture increases,  $BT_{8.6} - BT_{11}$  decreases while  $BT_{11} - BT_{12}$  increases.

$CO_2$  slicing (Smith and Platt 1978; Wylie and Menzel 1989) <sup>[12][13]</sup> is a useful method for sensing cloud amount and the height of clouds. Simple tests using the  $CO_2$  channels are useful for cloud mask, particularly high clouds. Whether a cloud is sensed by these bands (MODIS bands 33-36) is a function of the weighting function of the particular channel and the altitude of the cloud. MODIS band 35 (13.9  $\mu$  m) provides good sensitivity to the relatively cold regions of the atmosphere. Only clouds above 500 hPa will have strong contributions to the radiance to space observed at 13.9  $\mu$  m; negligible contributions come from the earth's surface. Thus a threshold test for cloud versus ambient atmosphere and a histogram test should reveal clouds above 500 hPa. This test will be used in conjunction with the near infrared thin cirrus test discussed.

Visible reflectance test is a single channel test whose strength is discriminating to bright clouds over dark surfaces (e.g., stratus over ocean) and weakness is clouds over bright surfaces (e.g., snow). Two different channels are used in this test dependent on the ecosystem. The 0.66  $\mu$  m (band 1) is used over oceans, land and snow/ice regions. The 0.88  $\mu$  m reflectance test is also applied over snow/ice and desert scenes.

The reflectance ratio test uses channel 2 divided by channel 1 ( $R_{0.87}/R_{0.66}$ ). This test makes use of the fact that the spectral reflectance at these two wavelengths is similar over clouds (ratio is near 1) and different over water and vegetation. Using AVHRR data this ratio has been found to be between 0.9 and 1.1 in cloudy regions. If the ratio falls within this range, cloud is indicated.

Clouds that are low in the atmosphere are often difficult to detect with infrared techniques. The thermal contrast between clear-sky and low cloud is small and sometimes undetectable. Reflectance techniques, including the reflectance ratio test can be applied during daylight hours

over certain ecosystems. Use of the MODIS band 18 at  $0.936 \mu\text{m}$  also offers help under daytime viewing conditions. Gao and Goetz (1991) proposed a ratio test using spectral channels near 0.94, 1.04, and  $1.14 \mu\text{m}$ . Reflectance of many surfaces is linear between these wavelengths while absorption by water vapor is different across this spectral region, allowing discrimination between cloud and the ground using a band ratio  $(R_{0.94} + R_{1.14})/2R_{1.04}$ . MODIS does not have channels at these three wavelengths; however, other water vapor channels in the near-infrared may prove useful for cloud detection over land. A reflectance ratio of band 18 over band 16 ( $0.865 \mu\text{m}$ , an atmospheric window with surface reflectance characteristics similar to channel 18) could be used.

The physical principle detecting snow using  $1.64 \mu\text{m}$  is the fact that the differences in reflected solar radiation between the  $0.645$  and  $1.64 \mu\text{m}$  bands contain information regarding cloud particle phase due to distinct differences in bulk absorption characteristics between water and ice at the longer wavelength. The visible reflectance, suffering no appreciable absorption for either ice or liquid water, is relatively unaffected by thermodynamic phase. However, if the cloud is composed of ice, or if the surface is snow covered (similar in effect to large ice particles), then the reflectance of the cloud at  $1.64 \mu\text{m}$  will be smaller than for an otherwise identical liquid water cloud.<sup>[11][12][13]</sup>

The detection of cloud shadows is a problem. Clear-sky scenes that are potentially affected by shadows can be theoretically computed given the viewing geometry, solar azimuth and zenith angles, cloud edges distribution and cloud altitude. This approach requires too much CPU, and all the information (e.g., cloud altitude) is not available to the cloud mask algorithm. Therefore, as with clouds, solar reflectance tests can be explored for a cloud shadow detection algorithm. For MODIS data, the cloud masking algorithm checks for shadows can be based on reflectance at  $0.94$ ,  $0.87$  and  $0.66 \mu\text{m}$ . A shadow is determined present if  $R_{0.936} < 0.12$  and  $R_{0.87}/R_{0.66} > 0.9$ <sup>[14][15]</sup>.

Over land during the day,  $BT_{3.9} > BT_{4.0}$  because there is more reflected solar energy at  $3.9 \mu\text{m}$ . In shadowed regions the incident solar radiation at  $3.9 \mu\text{m}$  is reduced, and the brightness temperature differences are smaller. The issues of shadows caused by mountainous terrain also need to study. These shadows would be directly calculable from digital elevation maps, solar geometry considerations, and the cloud mask. The first two considerations would indicate the field of view where terrain shadow could occur; the last would determine whether sunlight is available to cause the shadow<sup>[17]</sup>.

#### 4.2.2 CLOUD MASK AND CLOUD CLASSIFICATION TEST CASES

A simple cloud mask test is done using some thresholds as follows:  $BT_{11}$ ,  $BT_{11} - BT_{12}$ ,  $BT_{11} - BT_{8.6}$ ,  $BT_{13.9}$ ,  $R_{0.66}$ ,  $R_{0.87}$ ,  $R_{0.87}/R_{0.66}$ ,  $R_{1.6}$ . By applying one of these thresholds, a pixel will be classified as cloud or non-cloud. Different thresholds testing give different results. When multi-thresholds method is applied, pixel will be classified as cloud if most of the thresholds testing flag this pixel as cloud. After above processing, land-sea mask data is applied to imagery to distinguish the land and water body. Figure 3 is an example of the cloud mask using MODIS data over China (6 July 2001). The left image is composed image of band1, band2 and band4 and the right one is cloud mask image, green regions are land, blue regions are water, white areas are cloudy.

These thresholds,  $BT_{11}$ ,  $BT_{11} - BT_{12}$ ,  $R_{0.66}$ ,  $R_{1.6}$ ,  $BT_{13.9}$ , are used in the cloud classification test on the basis of cloud mask. Figure 4 is an example of the cloud classification using MODIS data



over China (6 July 2001). The left image is composed image of band1, band2 and band31 and the right one is cloud classified imagery. In cloud classified imagery, the green regions are land, blue regions are water, white cumulonimbus, cyan areas are cirrus, and dark yellow areas are low-level cloud. Over the Yangtse Rive drainage basin there are outer cloud system of the tropical cyclone.

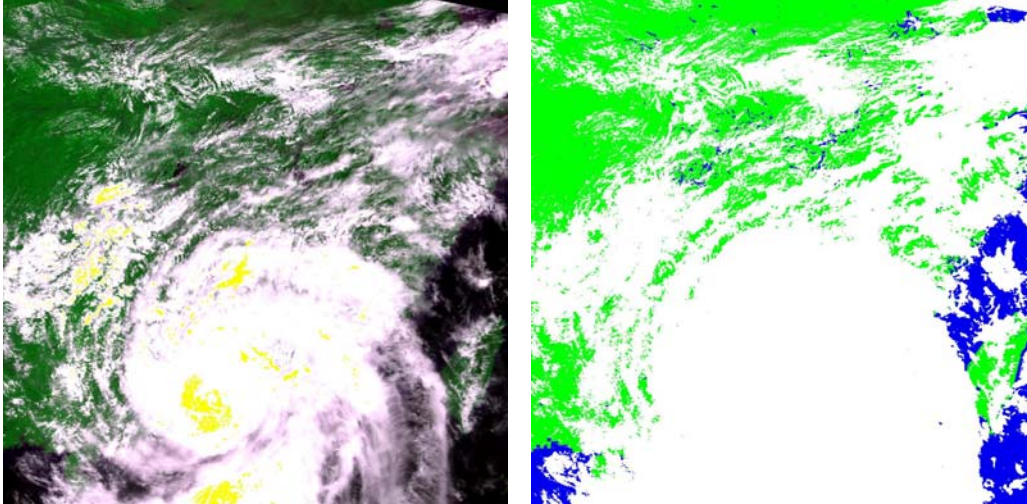


**Figure 3.** An example of the cloud mask using MODIS data over China (6 July 2001) .

The left image is combination by ch1/2/4 and the right one is cloud mask image, green regions are land, blue regions are water, white areas are cloudy.

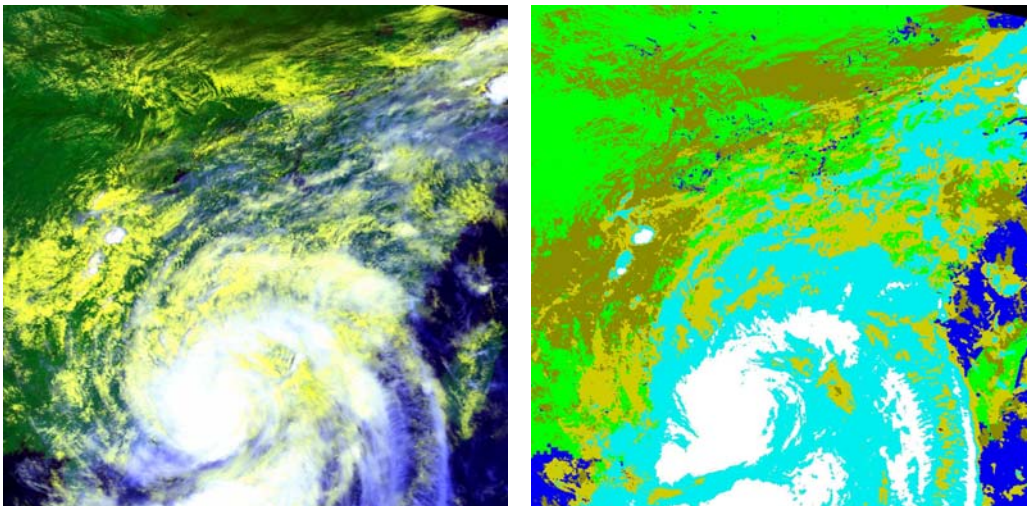


**Figure 4.** An example of the cloud classification using MODIS data over China (6 July 2001) .

The left image is composed image of band1, band2 and band31 and the right one is cloud classified imagery.

In cloud classified imagery, the green regions are land, blue regions are water, white cumulonimbus, cyan areas are cirrus, and dark yellow areas are low-level cloud.

## 5. CONCLUSION

This paper discussed cloud mask and cloud classification methods using the different satellite data. Some conclusions can be drawn from the study as follows:

- (1) The different cloud classification methods have their advantage and disadvantage. In this paper we discussed the automated pixel-scale neural network method, the automated 8\*8 pixels neural network method, and the automated pixel-scale multi-spectrum thresholds technique to detect and to classify clouds. For neural network cloud classification methods it has higher classification accuracy for one better sample database, but if some case did not occur in this sample database the neural network model can not recognize it. A perfect sample database that it includes almost all case in the different season and in the different area will need large resources. For pixel-scale multi-spectrum threshold technique it is relatively easy to adapt thresholds to varying meteorological conditions, earth surface types, viewing geometry using external data. One of the main disadvantages is that the thresholds need to be tuned frequently.
- (2) Using MODIS data, we can distinguish between cloud free and cloudy situation more exactly and recognize the different types of clouds more easily. Snow and low cloud is more easily distinguished using MODIS bands 6 (1.64  $\mu$  m), and bands 6 is helpful for distinguishing between the ice cloud and water cloud. MODIS has measurements at three wavelengths in the window, 8.6, 11, and 12  $\mu$  m, which are very useful in determination of cloud free atmospheres, and their combination are helpful in determining the thin cirrus.
- (3) It shows that using pixel-scale methods are more suitable for practical application than 8\*8 pixels scale methods through testing using AVHRR data. Although classification accuracy of 8\*8 pixels samples is a little better than single pixel sample, but when neural network model is used in the practical application for a satellite image single pixel cloud classification neural network model is better.
- (4) Although the spatial resolution of the GMS-5 data is lower than AVHRR and MODIS data, but its higher time resolution makes it reflect weather system evolution process better. It can show clearly that the meso-scale convective cloud clusters in the MEIYU front evolve with time.
- (5) Cloud mask result is the foundation of other studies such as SST and LST (land surface temperature), TPW (total precipitable water) retrieval and vegetation study using these satellite data. The output of cloud classification can be used to modify the NWP output cloud.

## 6. REFERENCES

1. P. M. Atkinson and A. R. L. Tatnall, (1997), Introduction: Neural networks in remote sensing, *Inter. J. Remote Sensing*, Vol.18, No.4, 699-710.
2. G. M. Foody and M. K. Arora, (1997), Remote sensing image analysis using a neural network and knowledge-based processing, *Inter. J. Remote Sensing*, Vol.18, No.4, 811-828.
3. Peak, J. E., and Tag, P. M. Segmentation of satellite imagery using hierarchical thresholding and neural networks. *J. Appl. Meteor.*, 33 (1994), 605-616.
4. Michel Desbois, Genevieve Seze and Gerard Szejwach, (1982), Automatic Classification of Clouds on METEOSAT Imagery: Application to High-Level Clouds, *J. Appl. Meteor.*, 21, 401-412.

5. Ackerman, S. A., W. L. Smith and H. E. Revercomb, (1990): The 27-28 October 1986 FIRE IFO cirrus case study: Spectral properties of cirrus clouds in the 8-12 micron window. *Mon. Wea. Rev.*, **118**, 2377-2388.
6. Hutchison, K. D., and K. R. Hardy, (1995): Threshold functions for automated cloud analyses of global meteorological satellite imagery. *Int. J. Remote Sens.*, **16**, 3665-3680.
7. Kriebel, K. T., and R. W. Saunders, (1988): An improved method for detecting clear sky and cloudy radiances from AVHRR data. *Int. J. Remote Sens.*, **9**, 123-150.
8. Spinhirne, J. D., W. D. Hart and D. L. Hlavka, (1996) Cirrus infrared parameters and shortwave reflectance relations from observations. *J. Atmos. Sci.*, **53**, 1438- 1458.
9. Strabala, K. I., S. A. Ackerman, and W. P. Menzel, (1994): Cloud properties inferred from 8-12  $\mu\text{m}$  data. *J. Appl. Meteor.*, **33**, 212-229.
10. Ackerman, S. A., W. L. Smith and H. E. Revercomb, (1990): The 27-28 October 1986 FIRE IFO cirrus case study: Spectral properties of cirrus clouds in the 8-12 micron window. *Mon. Wea. Rev.*, **118**, 2377-2388.
11. Strabala, K. I., S. A. Ackerman, and W. P. Menzel, (1994): Cloud properties inferred from 8-12  $\mu\text{m}$  data. *J. Appl. Meteor.*, **33**, 212-229.
12. smith, W. L., and C. M. R. Platt, 1978: Intercomparison of radiosonde, ground based laser, and satellite deduced cloud heights. *J. Appl. Meteor.*, **17**, 1796-1802.
13. Wylie, D. P., and W. P. Menzel, 1989: Two years of cloud cover statistics using VAS. *J. Clim* , **2**, 380-392.
14. Tsonis, A. A., (1984): On the separability of various classes from GOES visible and infrared data. *J. Clim. Appl. Meteor.*, **23** 1393-1410.
15. Yamanouchi, T., K. Suzuki, and S. Kawaguci, (1987): Detection of clouds in Antarctica from infrared multispectral data of AVHRR. *J. Meteor. Soc. Japan*, **65**, 949-962.
16. Gao, B.-C. and W. J. Wiscombe, 1994: Surface-induced brightness temperature variations and their effects on detecting thin cirrus clouds using IR emission channels in the 8-12 micron region. *J. Appl. Met.*, **33**, 568-570.
17. Rossow, W. B., A. W. Walker, and L. C. Garder, (1993): Comparison of ISCCP and other cloud amounts. *J. Climate*, **6**, 2394-2418.

# Proceedings of the Fourteenth International TOVS Study Conference

Beijing, China  
25-31 May 2005

